

# Enhanced synergism of antibiotics with zinc oxide nanoparticles against extended spectrum $\beta$ -lactamase producers implicated in urinary tract infections

Rashmi M. Bhande · C. N. Khobragade ·  
R. S. Mane · S. Bhande

Received: 12 July 2012 / Accepted: 29 December 2012 / Published online: 12 January 2013  
© Springer Science+Business Media Dordrecht 2013

**Abstract** In this study, enhanced synergistic bioactivity of zinc oxide nanoparticles (ZnO NPs) with  $\beta$ -lactam antibiotics were evaluated against a panel of clinically isolated extended spectrum  $\beta$ -lactamase producers implicated in urinary tract infections. Chemically synthesized zinc oxide nanoparticles (15 nm) were characterized by X-ray diffraction (XRD), scanning electron microscopy (SEM), high resolution transmittance electron microscopy (HR-TEM), selective area electron diffraction (SAED), X-ray photoelectron spectroscopy (XPS), and UV–Visible spectrophotometry techniques. The antimicrobial potency ( $10 \pm 0.66$ ,  $12$ ,  $11.33 \pm 1.10$ , and  $0.7 \pm 0.66$  mm inhibiting zone) and minimum inhibitory concentrations (80, 60, 30, 50  $\mu\text{g/ml}$ ) of ZnO NPs were tested separately whereas time–kill and membrane leakage assays were evaluated in combination with ZnO NPs+ cefotaxime, ampicillin,

ceftriaxone, cefepime against the  $\beta$ -lactamase producer strains of *E. coli*, *K. pneumoniae*, *S. paucimobilis*, and *P. aeruginosa*, respectively. Time–kill curve dynamics of ZnO NPs with  $\beta$ -lactam antibiotics revealed enhanced bactericidal activity (50, 85, 58, 50 % fold inhibition) by delaying the exponential and stationary phases of all isolates when tested separately. Posttime–kill effect was studied on cell membrane by assaying leakage of reducing sugars (130.2, 124.7, 137, and 115.8  $\mu\text{g/bacterial dry weight of 1 mg}$  ( $\mu\text{g/mg}$ ) and proteins (15, 10, 16, 18  $\mu\text{g/mg}$ ). These assays revealed that membrane leakage was due to synergism of ZnO NPs+  $\beta$ -lactam antibiotics which successfully damage cell membrane thereby leading to death of all ESBL producers. The results demonstrate the utilization of ZnO NPs as a potentiator of  $\beta$ -lactam antibiotics and suggest the possibility to use nanoparticles in a combination therapy to treat UTI.

R. M. Bhande · C. N. Khobragade (✉)  
School of Life Sciences, Swami Ramanand Teerth  
Marathwada University, Nanded 431 606, India  
e-mail: profcnkbt@rediffmail.com

R. M. Bhande  
e-mail: bhanderashmi@gmail.com

R. S. Mane · S. Bhande  
School of Physical Sciences, Swami Ramanand Teerth  
Marathwada University, Nanded 431 606, India  
e-mail: rsmene@rediffmail.com

S. Bhande  
e-mail: sambhajibhande@gmail.com

**Keywords** Zinc oxide nanoparticles ·  $\beta$ -Lactamase · Urinary tract infections · Drug–nanoparticle synergism

## Introduction

Despite of prodigious efforts, the continuous development of bacterial resistance to antibiotic treatment is still considered as a major drawback in chemotherapy for infectious diseases (Bennet 2008). Bacterial urinary tract infections (UTIs) are frequently

encountered in outpatients as well as nosocomial settings and categorized as the second most common infections in clinical practices (Nicole et al. 1988). Now-a-days clinicians recommend empirical therapy and use of broad spectrum  $\beta$ -lactam antibiotics that enable the UTI pathogens to produce variety of  $\beta$ -lactamases. Extended spectrum  $\beta$ -lactamases (ESBLs), predominantly produced by strains of *Enterobacteriaceae* family are proved to be the most important cause of bacterial resistance to  $\beta$ -lactam antibiotics like penicillins, cephalosporins, etc., and may cause serious therapeutic failure if not treated properly. Besides of antibiotic therapy, the morbidity and mortality associated with these bacterial infections remain high and hence the clinical efficacy of  $\beta$ -lactam antibiotic get compromised. Consequently it is a strong incentive to develop new bactericidal agents with novel antimicrobial mechanism.

Since a decade, nanotechnology merges the tailoring of materials at atomic level with unprecedented unique properties and can be manipulated for the desired applications (Gleiter 2000). At present nanoparticles are employed as a tool to explore the darkest avenues of medical sciences in several ways like imaging (Wren and Nie 1998), sensing (Vaseastha and Dimova-Malinovaska 2005), targeted drug delivery (Langer 2001), gene delivery system (Roy et al. 1999), and artificial implants. The high surface to volume ratio of nanoparticles allows a broader gamut of interactions with organic and inorganic molecules to impart its antibacterial effects (Kim et al. 2007). The role of metal–microbe interactions in several fields such as bioremediation, biomineralization, bioleaching, and microbial corrosion is well known (Bruins et al. 2000) but in case of nanotechnology microbe–nanoparticle–bimolecular interactions have yet to be explored adequately. Some recent studies indicated that antibiotic formulations based on nanoparticles are effective in controlling the outbreak of new multiple drug resistant *Staphylococcus aureus* (Tiller 2001). Thus the present scenario makes current research findings to develop stable, robust, and durable bactericidal nanoparticles on the basis of antibiotic formulations.

Due to the nanoscale size, inorganic nanoparticles have elicited much interest in medicines. Based on this aspect it is demonstrated that specific antibiotic formulation comprising metal oxide nanoparticules could be effective bactericidal materials (Pal et al.

2007). Moreover, there are extensive reports are available on antibacterial action of silver (Sharma et al. 2009), copper, tin, and titanium nanoparticles, etc., (Pen 2009) which are seldomly used in the antimicrobial industry. Among metal oxide nanoparticles the zinc oxide nanoparticle (ZnO NP) is one of the well-known versatile and technologically important multifunctional material due to its significant features like transparency in the visible range, environmental, and electrical stability, direct energy band-gap of 3.37 eV with a large excitation binding energy of 60 meV, environmental friendliness, nontoxicity, abundance in nature, high surface-to-volume ratio for better interactions with bacteria (Park et al. 2009) and ability to inhibit 100 % bacterial growth by accumulating intracellularly at very low concentration, i.e., 3–10 mM (Brayner et al. 2006). The bactericidal action is reported to be due to cell membrane disruption, UV induction of intracellular reactive oxygen species, i.e.,  $\text{H}_2\text{O}_2$ ,  $\text{OH}^-$ , and  $\text{O}_2^-$  (Jones et al. 2008). As of date, the process underlying their bactericidal effect is not clear. So it will be interesting to understand the mechanism of action of ZnO NPs against multidrug resistant microorganisms involved in infectious diseases like UTI. To understand better and investigate the inhibitory nature and lethal effects of ZnO NPs on multidrug resistant UTI pathogens in combination with  $\beta$ -lactam antibiotics we used a panel of potential ESBL producing strains as model organisms.

Up till now very few reports are available on synergistic bactericidal activity of inorganic nanomaterials in combination with  $\beta$ -lactam antibiotics and to the best of our knowledge synergistic activity of (ZnO NPs) nanoparticles with  $\beta$ -lactam antibiotics have not yet been thoroughly investigated. In this article, we attempted to evaluate the  $\beta$ -lactam antibiotic formulation based on ZnO NPs against a panel of ESBL producing strains in the presence and absence of their sub-inhibitory concentrations.

## Methods and materials

### Synthesis of ZnO nanoparticle (ZnO NP)

ZnO NPs were synthesized by low temperature sol–gel method. Basically, 0.09 g  $\text{Zn}(\text{CH}_3\text{COOH})_2$  and 0.12 g KOH were dissolved into 50 ml methanol and mixed rapidly while stirring at 1,000 rpm at 60 °C for 5 min

and then cooled to room temperature so as to obtain transparent solution of ZnO NPs. The resulting nanoparticles were then washed with triple-distilled water by using centrifugal method for several times to remove the organic impurities present in it. The ZnO NPs thus prepared were then annealed at 300 °C for the crystallinity improvement and used further for its structural, optical, and surface evaluation properties.

#### Isolation, identification and confirmation of ESBL producers

About 80 urine samples of clinically diagnosed UTI patients (7–40 years) were collected in the wide mouthed sterile plastic container (HiMedia) prior to antibiotic treatment and transported immediately to laboratory in an ice-cold condition by adding boric acid at a final bacteriostatic concentration of 1.8 % and used without delay (Maskell 1982).

For isolation of almost all uropathogens a loopful of urine sample was streaked on six different selected and differential growth media viz. Mac Conkey's agar, blood agar, CLED agar, Nutrient agar, UTI agar, and combinational agar (CLED + Mac Conkey's + Blood) and incubated at 37 °C for 24 h (Muhammad et al. 2004). After incubation colonies were selected and characterized on the basis of morphological, cultural, biochemical tests (Faddin 1980), and were identified by 16S rRNA technique.

Isolates were further subjected to ESBL confirmation by double disc synergy test (DDST) (Barbaru et al. 2008). In DDST, 0.5 Mac Farland turbidity adjusted bacterial test strains were swab inoculated on Muller–Hinton agar (HiMedia) and 3G cephalosporin, i.e., cefotaxime (30 µg), ceftazidime (30 µg) were placed 15 mm apart from a disk of amoxicillin (20/10 µg) which was placed at the center of a Petri-dish and incubated at 37 °C for 18–24 h. An enhanced zone of inhibition between any one of the β-lactam disc toward the augmentin disc was interpreted as presumptive evidence for the presence of ESBLs (CLSI 2000).

#### Bacterial susceptibility testing for ZnO NPs and standard β-lactam antibiotics

Synthesized ZnO NPs were tested for preliminary antimicrobial activity by agar well diffusion bioassay (Bauer et al. 1966). Tubes containing 7 ml nutrient

broth was inoculated with an overnight grown test cultures (*E. coli*, *K. pneumoniae*, *S. paucimobilis*, *P. aeruginosa*) until the density reaches to 0.5 Mac Farland turbidity standard (approximately 10<sup>5</sup> cfu/ml) and swab inoculated on sterile Muller–Hinton agar plates. Wells of 5 mm diameter were prepared by using cork borer in the pre solidified agar plates and 50 µl (0.002 mg) of ZnO NP solution was added into each well of all plates. Four different antibiotics specified for β-lactam class, i.e., cefotaxime, ampicillin, ceftriaxone, cefepime (HiMedia) were tested for the same on separate MHA plates and incubated at 37 °C for 24 h. The sensitivity of isolate toward each antimicrobial agent and ZnO NP was measured and recorded. The *E. coli* ATCC 25922 was used as a positive control.

#### MIC of ZnO NPs and β-lactam antibiotics

Minimum inhibitory concentration (MIC) of β-lactam antibiotics and ZnO NPs were determined separately and in combination by tube dilution method. Inocula was prepared by growing test strains in Muller–Hinton broth at 37 °C until bacterial count reaches to 10<sup>8</sup>–10<sup>9</sup> CFU/ml. The cultures were filtrated twice and the cells were washed with phosphate buffer (pH 7) and further suspended in distilled water until the inocula reached approximately to 5.0 × 10<sup>6</sup> CFU/ml. Four isolated bacterial cells aliquot was incubated in test tube containing 7 ml Muller–Hinton broth with concentration ranging from 240 to 0.001 µg/ml for cefotaxime, ampicillin, ceftriaxone, cefepime and concentration of 0–120 µg/ml for ZnO NPs at 37 °C for 24 h. After 24 h MICs of cefotaxime, ampicillin, ceftriaxone, and cefepime as well as ZnO NPs were determined.

To get MIC of the combination, i.e., antibiotics and ZnO NP against each strain, the cells were inoculated in MHB and incubated under following different combinations viz: cefotaxime (240 µg/ml) + ZnO NPs (10 µg/ml), cefotaxime (240 µg/ml) + of ZnO NPs (20 µg/ml), ampicillin (120 µg/ml) + ZnO NPs (10 µg/ml), ceftriaxone (60 µg/ml) + ZnO NPs (40 µg/ml), cefepime (20 µg/ml) + ZnO NPs (60 µg/ml) instead of single antibiotic or ZnO NP alone. To eliminate other random factors all assays were carried out in three duplicates to determine the accurate MIC of antibiotics and ZnO NPs in combination and individually.

## Time–kill curve

Time–kill synergy assay (Raffi et al. 2008; Gaddad and co-workers 2010) was carried out to find the enhanced antibacterial effect of ZnO NPs against isolated ESBL producers. *E. coli*, *K. pneumoniae*, *S. paucimobilis*, and *P. aeruginosa* were grown at the concentration of  $10^8$  cells/ml in a 250 ml Muller–Hinton broth supplemented with a 1/2 MIC of ZnO NPs + 1/2 MIC of each cefotaxime, ampicillin, ceftriaxone, cefepime separately. For *E. coli* 1/2 MIC of ZnO NP (80  $\mu\text{g/ml}$ ) + 1/2 MIC of cefotaxime, ampicillin, ceftriaxone, cefepime (0.016; 0.001; 0.0256, and 1.024  $\mu\text{g/ml}$ ), respectively. For *K. pneumoniae* 1/2 MIC of ZnO NPs (60  $\mu\text{g/ml}$ ) + 1/2 MIC of cefotaxime, ampicillin, ceftriaxone, cefepime (0.032; 0.1; 0.124; 0.001  $\mu\text{g/ml}$ ), respectively, was taken. For *P. aeruginosa* 1/2 MIC of ZnO NPs (30  $\mu\text{g/ml}$ ) + 1/2 MIC of cefotaxime, ampicillin, cefotaxime, cefepime (2; 0.064; 0.064; 0.001  $\mu\text{g/ml}$ ), respectively, was taken. For *S. paucimobilis* 1/2 MIC of ZnO NPs (50  $\mu\text{g/ml}$ ) + 1/2 MIC of cefotaxime, ampicillin, ceftriaxone, and cefepime (0.051; 256; 0.0256; 0.1  $\mu\text{g/ml}$ ) was prepared, respectively. All above cited combinations were incubated at 37 °C. The negative control was maintained with nanoparticles while antibiotics individually. Growth rates of bacterial species were assessed at every 30 min interval by measuring absorbance (OD) at 600 nm (Shimadzu, Japan).

## Bacterial membrane leakage assay

To examine the posttime–kill (Synergy) effect of ZnO NPs+  $\beta$ -lactam antibiotics on ESBL producers the membrane leakage assay was performed by estimating the amount of reducing sugars and proteins. In different volumes of MH broth (10 ml), ZnO NPs and *E. coli*, *K. pneumoniae*, *S. paucimobilis*, *P. aeruginosa* cells ( $5 \times 10^5$  cfu/ml) were added separately with concentrations corresponding to time–kill experiments with respect to each organism. The cultures were incubated at  $37 \pm 2$  °C with continuous shaking at 150 rpm. For 2–4 h about 1 ml culture was sampled out from inoculated broth containing ZnO NPs. The sample was centrifuged at 12,000 rpm, supernatant collected and immediately frozen at 4 °C. The concentration of reducing sugars and proteins were determined by standard methods (Bradford 1976; Miller 1959). Control experiments were conducted in the absence of ZnO NPs and  $\beta$ -lactam antibiotics.

## Results and discussion

### Structural elucidation and morphological evaluation of synthesized ZnO NPs

The XRD analysis (Fig. 1) clearly revealed the sharp and distinct peaks. These peaks were analyzed with JCPDS data file 05-0664 and confirmed the presence of pure crystalline ZnO. No peaks corresponding to zinc metal was detected indicating that the deposited ZnO NPs are highly pure in phase. The four peaks in XRD correspond to (100), (002), (101), and (103) reflections. The average grain size as calculated by using Scherer formula from first three peaks is  $\sim 15$  nm.

Surface morphological study was carried out using field-emission scanning electron microscopy (SEM) images. The synthesized ZnO NPs were dispersed in water with 50 % w/v and subjected to ultrasonic treatment for 3 h so as to remove the agglomeration if present in the dispersion. The resulting dispersion then spin-coated on to a cleaned glass slide for the scanning electron microscopy wherein, a uniform growth of ZnO spherical nanoparticles were obtained. Moreover, the ZnO NP film was free from the agglomeration effect indicating high dispersion rate in water (Fig. 2a). To confirm the crystal size estimated by using XRD analysis, transmission electron microscopy images (TEM) have been taken at two different magnifications (Fig. 2b, c). The High magnified TEM image taken at 5 nm magnification (Fig. 2c) shows the lattice fringes indicating particle orientation, size, and grain boundaries. Thus, the particle size by using XRD is confirmed as  $\sim 15$  nm in diameter. The SAED

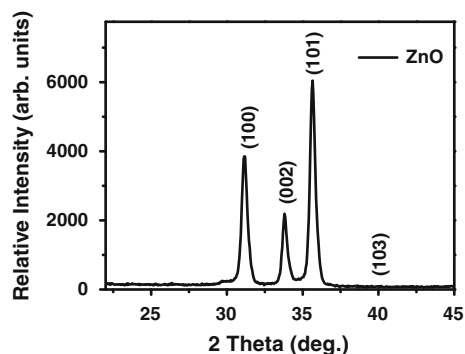


**Fig. 1** The XRD pattern of ZnO NPs

(selective area electron diffraction) pattern also shows the highly crystalline nature of ZnO NPs (Fig. 2d).

#### Surface and optical analysis of synthesized ZnO NPs

A sensitive surface analysis technique, X-ray photoelectron spectroscopy (XPS) was used to estimate contribution of Zn and O elements. The XPS data showed a binding energy peak position at about 531 eV corresponding to O (1s). The peak on the low binding energy side of the O (1s) spectrum released  $O^{2-}$  ions in the wurtzite structure of the hexagonal  $Zn^{2+}$  ion array was surrounded by zinc atoms with the full supplement of nearest neighbor  $O^{2-}$  ions. Accordingly, the peak of O 1s spectrum can be attributed to the Zn–O bonds. The higher binding energy at 531.96 eV is to the chemisorbed and dissociated oxygen and OH species on the surface of the ZnO thin film (Wang et al. 2006; Major et al. 1986). The Zn 2p at 1,022 eV is also noticed (Fig. 3).

The optical absorption measurement of ZnO NPs film was recorded within 300–900 nm wavelength range by UV–Visible spectrum. The absorbance versus wavelength plot shows ZnO NPs are transparent in the visible range. Sharp absorbance edge at  $\sim 390$  nm wavelength, corresponds to the bandgap energy of ZnO, i.e., 3.17 eV (Fig. 4).

#### Isolation, identification and confirmation of ESBLs

All the collected 80 urine samples were analyzed for isolation and identification of uropathogens by standard methods. Total 71 samples were found to be prominent bacteriurea in comparison with remaining samples (nonsignificant bacteriurea or very low bacterial count). In this study, for isolation of uropathogens six different growth media and one combination media (CLED agar + Mac Conkeys agar + blood agar) were used at one and the same time (Muhammad et al. 2004). Maximum numbers of isolates were

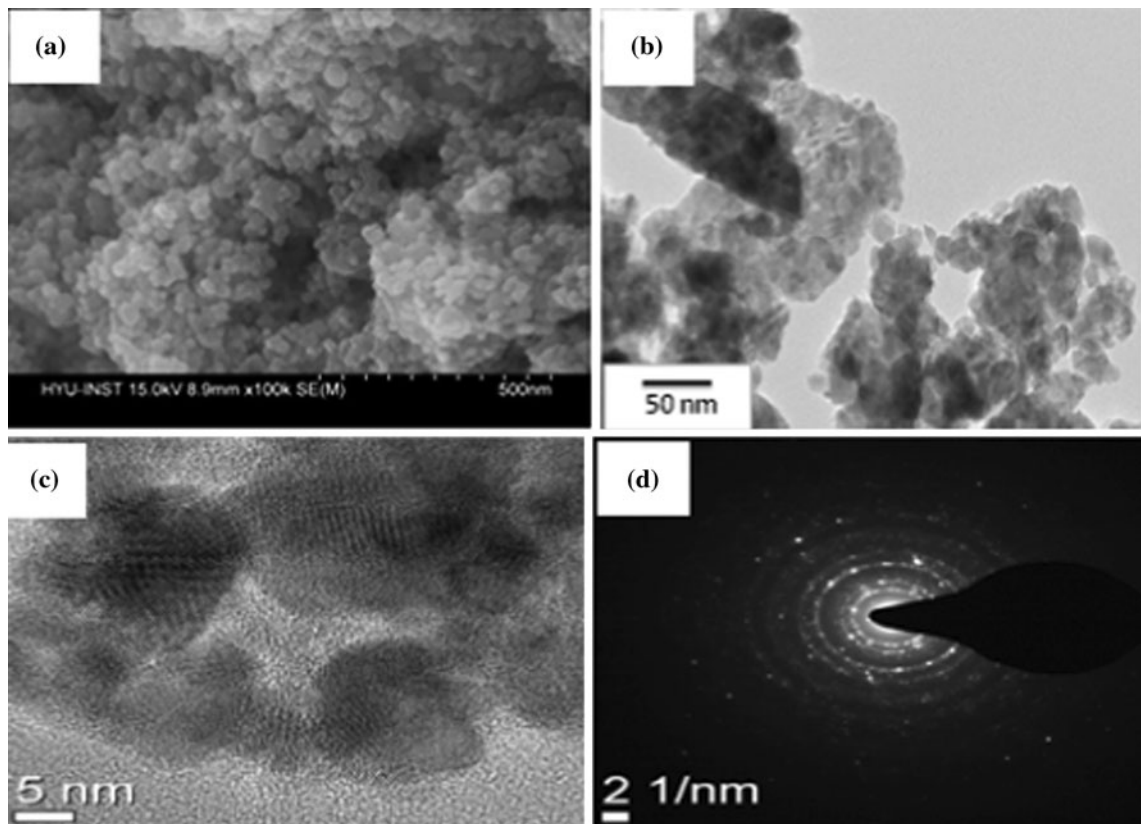


**Fig. 2** The SEM image of as-synthesized ZnO NPs

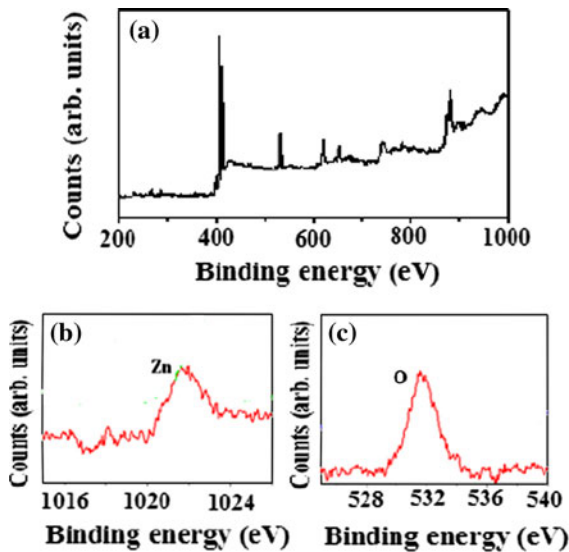


**Fig. 3** XPS spectra of ZnO NPs (a–c represent the scan over wide range and magnified band structure at Zn and O level)

obtained from combined media as compared to the single media (Graph 1). Combination of three agars, i.e., Mac Conkeys, blood, and CLED at one and same time had given 100 % detection rate of uropathogens in less efforts. From 71 uropathogens the bacterium *E. coli* (50 %) was found to be most common and prominent isolate followed by *K. pneumoniae* (30 %), *S. paucimobilis* (1 %), and *P. aeruginosa* (19 %) (Fig. 5). To our knowledge UTI causing and ESBL producing *S. paucimobilis* has not been reported so far. All the four isolates revealed the enhanced zone of inhibition greater than 5 mm toward the augmentin disc and hence confirmed as ESBL producers and used for further experiments (Fig. 6).

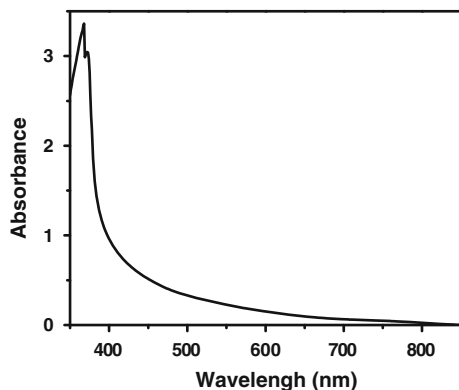
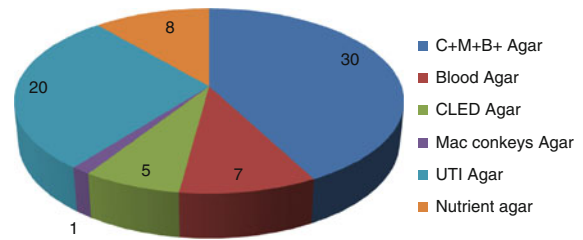


**Fig. 4** UV–Visible spectrum of ZnO NPs



**Graph 1** Number of isolates from different isolation media

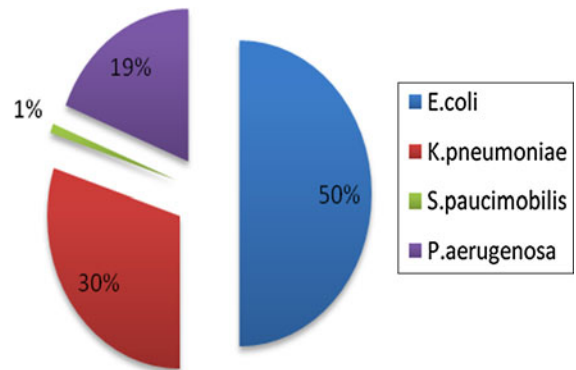


**Fig. 5** Percent occurrence and distribution of bacterial pathogens in UTI among the patients

#### Bacterial susceptibility testing

Preliminary qualitative antibacterial assessment (agar well diffusion test) revealed that ZnO NPs exhibited significant inhibitory activity on MDR *E. coli* (10 mm), *K. pneumoniae* (12 mm), *S. paucimobilis* (11 mm), and *P. aeruginosa* (0.7 mm), respectively, under laboratory conditions. All the four bacteria were proved to be resistant to four standard  $\beta$ -lactam antibiotics tested (Table 1). The inhibitory zone clearly imparts membrane disrupting biological activity of ZnO NPs. The mechanism by which the ZnO NPs are able to penetrate into bacteria is not understood completely, but it is hypothesized that when bacterial cell is treated with ZnO NPs then membrane morphology get changed significantly by increasing membrane permeability which facilitate proper transport of ZnO NPs through the bacterial plasma membrane resulting into cell death (Marones et al. 2005). Another reason might be the induction of intracellular reactive oxygen species including hydrogen peroxide ( $H_2O_2$ ) a strong oxidizing agent reported to be harmful to bacterial cells (Jones et al. 2008; Sawai 2003). The ZnO get activated by UV and

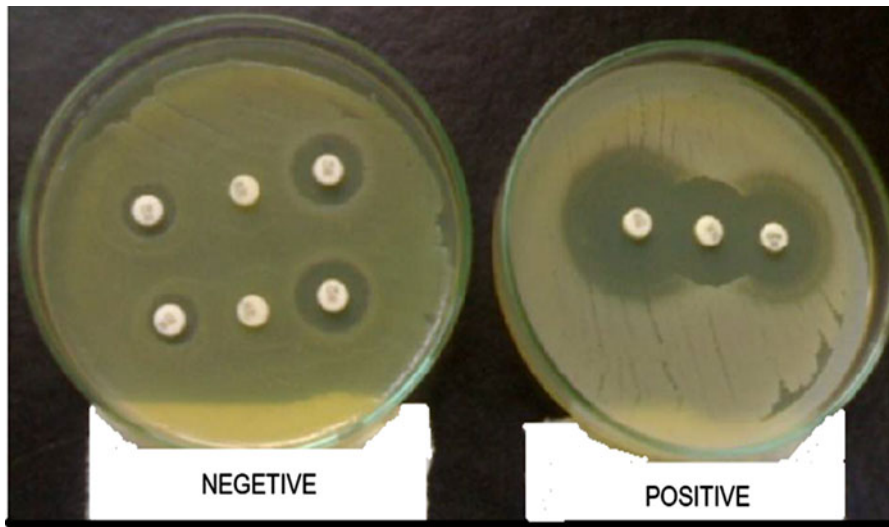


**Fig. 6** Confirmation of  $\beta$ -lactamase producers

Visible light and in a process of activation it generates highly reactive oxygen species such as  $\text{OH}^-$ ,  $\text{H}_2\text{O}_2$ , and  $\text{O}_2^{2-}$ . The negatively charged hydroxyl radicals and superoxides can not penetrate into cell membrane as such get agglomerate on the cell surface, whereas  $\text{H}_2\text{O}_2$  efficiently penetrate into cell membrane actively to disrupt the membrane and leads to bacterial cell death (Padmavathy and Vijayaraghvan 2008). The small particle size and larger surface area of ZnO NPs may also enhance antibacterial effect and exert cytotoxicity to microorganisms (Baker et al. 2005).

**Determination of MIC for ZnO NPs and  $\beta$ -lactam antibiotics**

Significant MIC values were obtained for ZnO NPs when tested alone and in combination against *E. coli* (80  $\mu\text{g/ml}$ ), *K. pneumoniae* (60  $\mu\text{g/ml}$ ), *P. aeruginosa* (30  $\mu\text{g/ml}$ ), *S. paucimobilis* (50  $\mu\text{g/ml}$ ) and standard  $\beta$ -lactam class antibiotics, i.e., cefotaxime (0.016, 0.032, 2, 0.051  $\mu\text{g/ml}$ ), ampicillin (0.001, 0.1, 0.064, 2.256  $\mu\text{g/ml}$ ), ceftriaxone (0.025, 0.1, 0.064, 0.025  $\mu\text{g/ml}$ ), and cefepime (1.024, 0.001, 0.001, 0.1  $\mu\text{g/ml}$ ) of results indicates that MIC values less than the values indicated above do not revealed significant antimicrobial effect on ESBL producers as  $P < 0.05$  (Table 2).

The multiple MIC combination of antibiotics and ZnO NPs were tested against a panel of ESBL producers as a prerequisite for time-kill assay. For

**Table 1** Antimicrobial susceptibility testing of ZnO NPs against UTI pathogens

Strains	ZnO nanoparticles ZnO NPs ZOI (mm)	Antibiotics			
		CF ZOI (mm)	A	CI	CPM
<i>E. coli</i>	10 $\pm$ 0.66	13	12	9	10
<i>K. pneumoniae</i>	12 $\pm$ 0.00	7	5	7	14
<i>S. paucimobilis</i>	11.33 $\pm$ 1.10	10	6	8	11
<i>P. aeruginosa</i>	0.7 $\pm$ 0.66	12	10	11	8

The data are shown as mean  $\pm$  SD  $< 0.05$

ZnO NPs zinc oxide nanoparticles, CF cefotaxime, A ampicillin, CI ceftriaxon, CPM cefepime, ZOI zone of inhibition

*E. coli* 0.016  $\mu\text{g/ml}$  cefotaxime + 80  $\mu\text{g/ml}$  ZnO, 0.001  $\mu\text{g/ml}$  ampicillin + 80  $\mu\text{g/ml}$  ZnO, 0.0256  $\mu\text{g/ml}$  + 80  $\mu\text{g/ml}$  ZnO NPs and 1.024  $\mu\text{g/ml}$  Ceftriaxon + 80  $\mu\text{g/ml}$  ZnO NPs were used in combination. These MIC values were seems to be promising as values lower than these ranges has no significant bactericidal effect. For, *K. pneumoniae* 0.032  $\mu\text{g/ml}$  cefotaxime + 60  $\mu\text{g/ml}$  ZnO NPs, 0.1  $\mu\text{g/ml}$  ampicillin + 60  $\mu\text{g/ml}$  ZnO NPs, 0.1  $\mu\text{g/ml}$  ceftriaxon + 60  $\mu\text{g/ml}$  ZnO NPs, and 0.001  $\mu\text{g/ml}$  cefepime + 60  $\mu\text{g/ml}$  ZnO NPs were confirmed as MIC values. For *P. aeruginosa* 2  $\mu\text{g/ml}$  cefotaxime + 30  $\mu\text{g/ml}$  ZnO NPs, 0.064  $\mu\text{g/ml}$  ampicillin + 30  $\mu\text{g/ml}$  ZnO NPs, 0.064  $\mu\text{g/ml}$  ceftriaxon + 30  $\mu\text{g/ml}$  ZnO NPs and 0.001  $\mu\text{g/ml}$

**Table 2** Minimum inhibitory concentration (MIC) of ZnO NPs and  $\beta$ -lactam antibiotics against UTI pathogens

	S. no.	Strains	MIC ( $\mu\text{g/ml}$ )				
			ZnO NPs	Std. antibiotics			
				CE	AM	CI	CPM
	1.	<i>E. coli</i>	80	0.016	0.001	0.0256	1.024
<i>ZnO NPs</i> zinc oxide nanoparticles, <i>CF</i>	2.	<i>K. pneumoniae</i>	60	0.032	0.1	0.1	0.001
cefotaxime, <i>AM</i> ampicillin, <i>CI</i>	3.	<i>P. aeruginosa</i>	30	2	0.064	0.064	0.001
ceftriaxon, <i>CPM</i> cefepime	4.	<i>S. paucimobilis</i>	50	0.051	256	0.025	0.1

cefepime + 30  $\mu\text{g/ml}$  of ZnO NPs were ideal MIC ranges. In case of *S. paucimobilis* the MIC combinations used were 0.051  $\mu\text{g/ml}$  cefotaxime + 50  $\mu\text{g/ml}$  ZnO NPs, 256  $\mu\text{g/ml}$  ampicillin + 50  $\mu\text{g/ml}$  ZnO NPs, 0.0256  $\mu\text{g/ml}$  ceftriaxone + 50  $\mu\text{g/ml}$  ZnO NPs, and 0.1  $\mu\text{g/ml}$  cefepime + 50  $\mu\text{g/ml}$  ZnO NPs. These effective combinations were further subjected to time–kill assays.

#### Time–kill curve

The dynamics of time–kill assay was monitored in both ways, i.e., broth dilution and agar diffusion method (% fold inhibition) for a panel of ESBL producers by synergistic manner (ZnO NPs+  $\beta$ -lactam antibiotics). Concentrations of MIC combinations (ZnO NPs+  $\beta$ -lactam antibiotics) discussed above were used for time–kill assay. It is noteworthy that all pathogens delayed the exponential phase of *E. coli*, *P. aeruginosa*, *S. paucimobilis*, and *K. pneumoniae* ( $10 \times 10^5$  cfu/ml) when treated with antibiotic and ZnO NPs separately than the normal exponential growth of pathogens (without nanoparticles and antibiotics).

When *E. coli* ( $5 \times 10^5$  cfu/ml) were treated with 0.016  $\mu\text{g/ml}$  cefotaxime, 0.001  $\mu\text{g/ml}$  ampicillin, 0.0256  $\mu\text{g/ml}$  ceftriaxone and 1.024  $\mu\text{g/ml}$  cefepime the exponential phase get delayed similar to that of ZnO NPs (80  $\mu\text{g/ml}$ ) but when the same *E. coli* were treated with combination of cefotaxime + ZnO NPs (0.016 + 80  $\mu\text{g/ml}$ ), ampicillin + ZnO NPs (0.001 + 80  $\mu\text{g/ml}$ ), ceftriaxone + ZnO NPs (0.025 + 80  $\mu\text{g/ml}$ ), and cefepime + ZnO NPs (1.024 + 80  $\mu\text{g/ml}$ ) there was sudden decrease in exponential phase duration and growth transition took place from the exponential to a very low Stationary phase (Fig. 7; The purple colored line indicates the time–kill curve of various  $\beta$ -lactam antibiotics (cefotaxime,

ceftriaxone, ampicillin, cefepime separately. To avoid the figure complexity here we have presented the single purple line instead of four independent lines). As per our findings *E. coli* is detected as potent (50 %) ESBL producers among all UTI pathogens and therefore cefepime + ZnO NPs or ampicillin + ZnO NPs synergy therapy may be helpful insight to treat this bug. A more probable cause of this synergism may be the action of ZnO NPs as a drug carrier into *E. coli* cell membrane with standard  $\beta$ -lactam antibiotics. To our knowledge cell membrane consist of hydrophobic group, i.e., phospholipids and glycoproteins and being hydrophilic in nature ZnO NPs approaches toward *E. coli* membrane, increases membrane permeability and facilitate the transfer of ampicillin (ampicillin is hydrophobic in nature) and cefepime into the cell membrane which finally leads to bacterial cell death.

In case of *K. pneumoniae*, the synergy of cefotaxime + ZnO NPs (0.016 + 60  $\mu\text{g/ml}$ ) and Ceftriaxone (0.1 + 60  $\mu\text{g/ml}$ ) suddenly decreased the duration of exponential as well as stationary phase and growth transition took place to a very low linear stationary phase (Fig. 8; The purple colored line indicates the time–kill curve of various  $\beta$ -lactam antibiotics (cefotaxime, ceftriaxone, ampicillin, cefepime separately. To avoid the figure complexity here we presented the single purple line instead of four independent lines.) The synergy of ampicillin + ZnO NPs and cefepime + ZnO NPs efficiently delayed the exponential phase. This increased antibacterial activity of ampicillin, cefepime, cefotaxime, and ceftriaxone was due to bonding reaction between antibiotic and ZnO NPs. The antibiotic molecule contains many active hydroxyl, amido groups which can react easily with ZnO NPs by chelation and cell surface interactions, so whenever antimicrobial group act on the point of increased surface of bacterial cells the more destruction of bacterial cell takes place and hence the



**Fig. 7** Time–kill curve of *E. coli* after treatment with ZnO NPs+  $\beta$ -lactam antibiotics

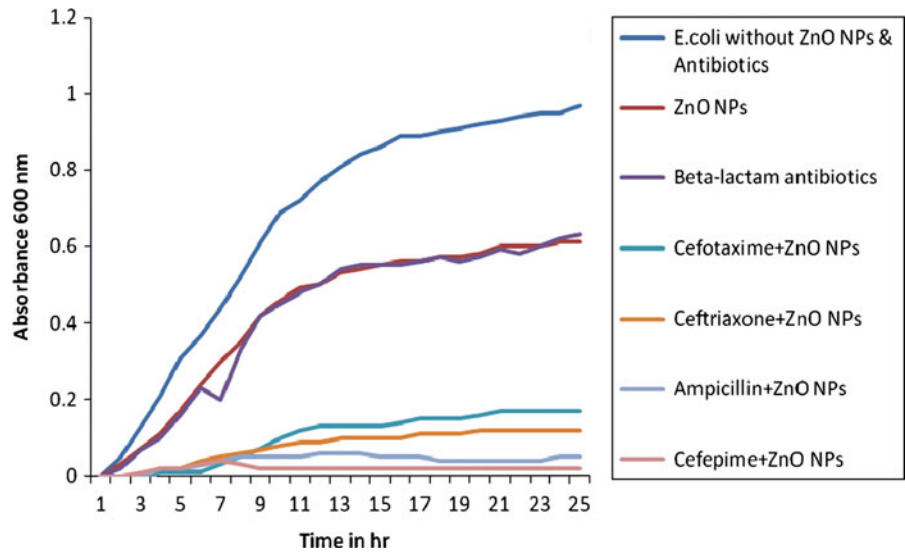
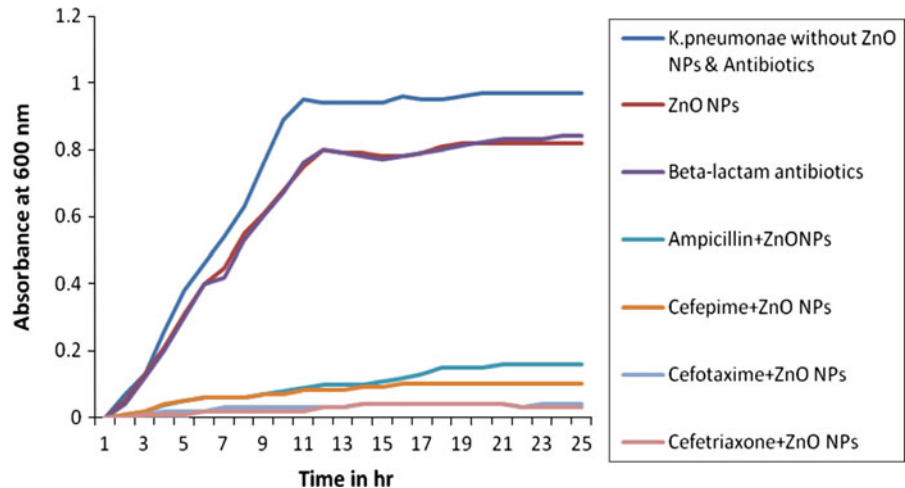


**Fig. 8** Time–kill curve of *K. pneumoniae* after treatment with ZnO NPs+  $\beta$ -lactam antibiotics



cefotaxime + ZnO NPs (0.032 + 60  $\mu\text{g/ml}$ ) and (0.1 + 60  $\mu\text{g/ml}$ ) concentrations might be an effective alternative to treat such bacterial infections.

The dynamics of time–kill assay revealed near about similar synergy pattern in both the bacteria, i.e., *P. aeruginosa* and *S. paucimobilis* (Figs. 9, 10). The green colored line indicates the time–kill curve of various  $\beta$ -lactam antibiotics (cefotaxime, ceftriaxone, ampicillin, cefepime separately. To avoid the figure complexity here we presented the single green line instead of four independent lines). No doubt here all combinations exerted good synergistic inhibition but in *P. aeruginosa* ceftriaxone + ZnO NPs and in *S. paucimobilis* ceftriaxone + ZnO NPs and cefepime + ZnONPs were proved to be potent one and thus

these combinations might be helpful in improvement of drug therapy related to these bacterial infections.

In this study, the synergy of ceftriaxone + ZnO NPs potentially inhibited almost all ESBL producers except *E. coli*. It is satisfactory that being a 3G cephalosporin, ceftriaxone therapy formulated with ZnO NPs can bring a new avenue for UTI treatment. Time–kill dynamics confirm that combination of 3G cephalosporins with ZnO NPs resulted into a greater bactericidal effect on all ESBL producers than either of antibacterial agents applied alone. An explanation for this increased synergistic activity would be based on assumption that ZnO NPs may interfere with the pumping activity of Nor A protein of *E. coli*, *P. aeruginosa*, and *K. pneumoniae*. The Nor A protein

**Fig. 9** Time–kill curve of *S. paucimobilis* after treatment with ZnO NP+  $\beta$ -lactam antibiotics

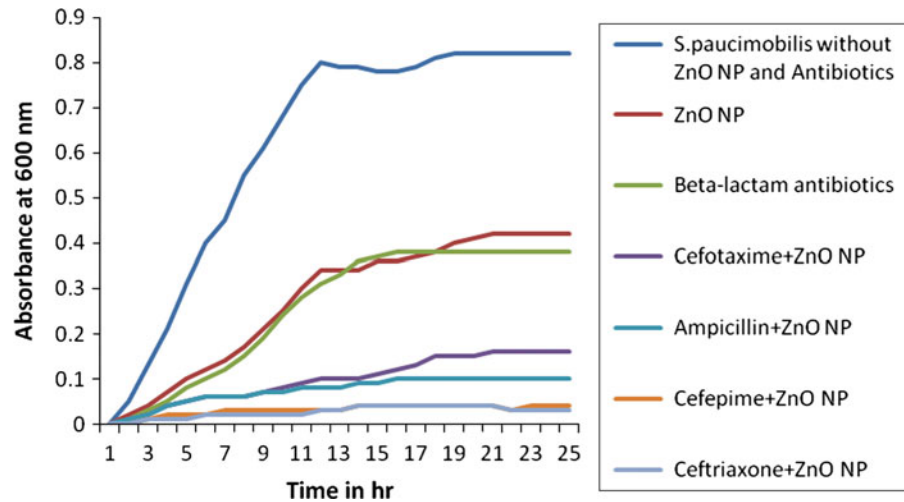
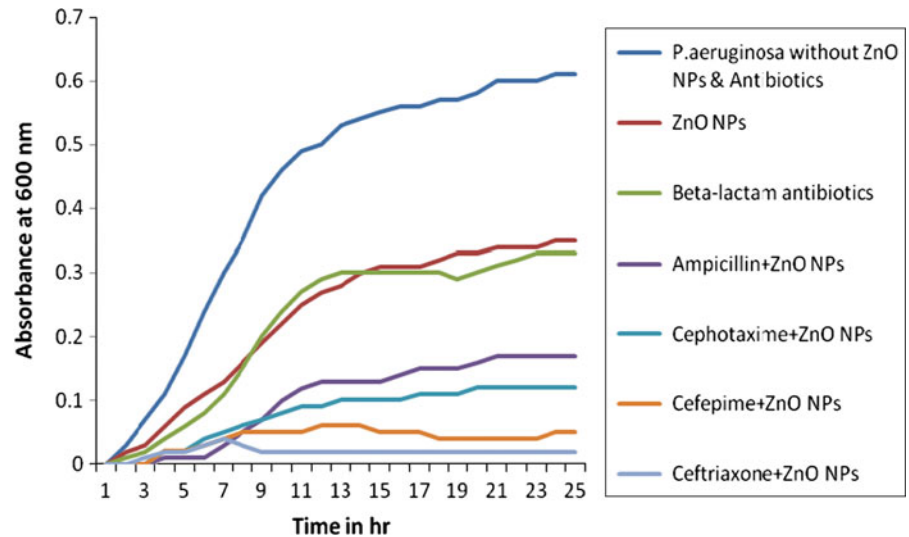


**Fig. 10** Time–kill curve of *P. aeruginosa* when treated with ZnO NPs+  $\beta$ -lactam antibiotics



mediates the active efflux of hydrophilic cefotaxime, ampicillin, ceftriaxone, cefepime from bacteria by conferring resistance upon the organism (Huet et al. 2008; Yu et al. 2002). ZnO NPs possess the ability to induce faster electron transfer kinetics in active site of enzyme (Kumor and Chen 2008; Huang et al. 2009) by interfering the pumping activity of this protein. There are reports (Ryan et al. 2001) suggesting that ZnO NPs may interfere with efflux pump system as well as may enhance the absorption of antibiotics into cell membrane by mediating omf proteins by improving their performance (Fernandez et al. 2007).

It is known that cefotaxime, ampicillin, ceftriaxone, and cefepime are member of cephalosporins and aminopenicillins which inhibits bacterial cell wall synthesis via competitive inhibition of the transpeptidase enzyme (an

enzyme responsible for bacterial cell wall synthesis). Thus considering the nitrogen atoms in  $\beta$ -lactam ring of ampicillin, ceftriaxone, cefotaxime, cefepime, and the hydroxylated surface (Noei et al. 2008) of ZnO NPs, the ampicillin–ZnO NPs, ceftriaxone–ZnO NPs, cefepime–ZnO NPs, and cefotaxime–ZnO NPs system may get stabilized through the ionic interaction network between protonated nitrogen atoms of  $\beta$ -lactam antibiotics and hydroxylated surface of ZnO NPs.

To assess accuracy of time–kill assay these concentrations were further subjected to agar plates for percent fold inhibition (Table 3). ZnO NPs (0.002 mg/ml), different antibiotics (cefotaxime, ampicillin, ceftriaxone, and cefepime (30  $\mu$ g/ml) and synergistic combination of each antibiotic related to respective organism was evaluated. The diameters of inhibition

**Table 3** Mean zone of inhibition with and without ZnO NPs against ESBL producers (synergy study)

Strains	Antibiotic	(Zone of inhibition in mm)			
		ZnO NPs (A)	Antibiotic	ZnO NPs + antibiotic (B)	Fold increase $\frac{(B-A)}{A} \times 100$ (%)
<i>E. coli</i>	Cephotaxime	10	13	17	30.76
	Ampicillin		12	18	50.00
	Ceftriaxone		9	12	33.33
	Cefepime		10	15	50.00
<i>K. pneumoniae</i>	Cephotaxime	12	7	13	85.71
	Ampicillin		5	7	40.1
	Cefepime		7	11	57.14
	Ceftriaxone		14	26	85.71
<i>S. Paucimobilis</i>	Cephotaxime	11.33	10	11	10
	Ceftriaxone		6	9	50
	Cefepime		8	12	50
	Ampicillin		11	13	18.18
<i>P. aeruginosa</i>	Cephotaxime	0.7	12	19	58.33
	Ceftriaxone		10	7	70.00
	Ampicillin		11	14	27.27
	Cefepime		8	12	50.00

zones (mm) in the presence or absence of ZnO NPs and in combination were measured. The increase in percent fold inhibition of Cefotaxime with ZnO NPs against all ESBL producers were almost similar to the time–kill assay, i.e., 85.7, 50, 70, 33 % for *K. pneumoniae*, *S. paucimobilis*, *P. aeruginosa*, and *E. coli*, respectively. As these antibiotics are implicated in cell wall lysis mechanism and bind each other by Van der Waals interactions, the antimicrobial groups comes into contact with ZnO NPs where the ZnO core surrounded by antibiotics makes action on bacterial cell wall and lead to cell lysis by increasing penetration of ZnO NPs into bacterium. The ZnO NPs–antibiotic complex reacts with DNA and prevent DNA unwinding by resulting into serious damage to bacterial cell (Ping et al. 2005). These facts could provide the possible explanation for enhancement of synergistic antibacterial mechanism.

Membrane leakage assay

To assess the time–kill results on bacterial membrane and to analyze the bactericidal activity by increase in membrane permeability membrane leakage assay was performed (Li et al. 2009). Results revealed that ZnO NPs could enhance membrane permeability by leakage of reducing sugars (Fig. 11). Initially in control no

reducing sugar was detected at all but when the cells were treated with ZnO NPs + β-lactam antibiotics combination the leaked reducing sugar amount was estimated to be 32.3, 28.6, 35.7, and 25.5 μg/bacterial dry wt. of/mg (μg/mg) for *E. coli*, *K. pneumoniae*, *P. aeruginosa*, and *S. paucimobilis*, respectively. After 24 h treatment the leakage amount increased up to 130.2, 124.7, 137, and 115.8 μg/bacterial dry weight of 1 mg (μg/mg) suggesting that these combinations

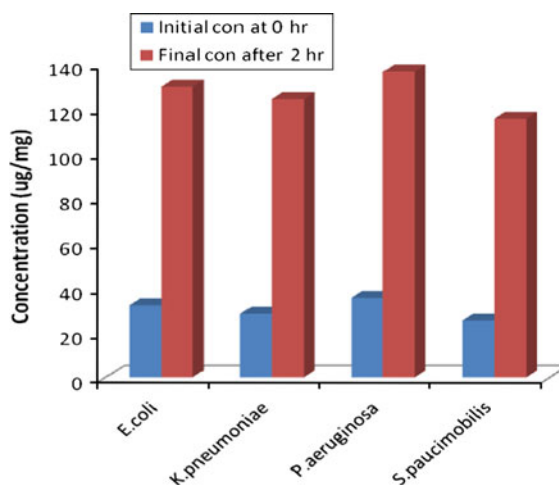


**Fig. 11** Leakage of reducing sugars from ESBL producers after the treatment of ZnO NPs+ β-lactam antibiotics

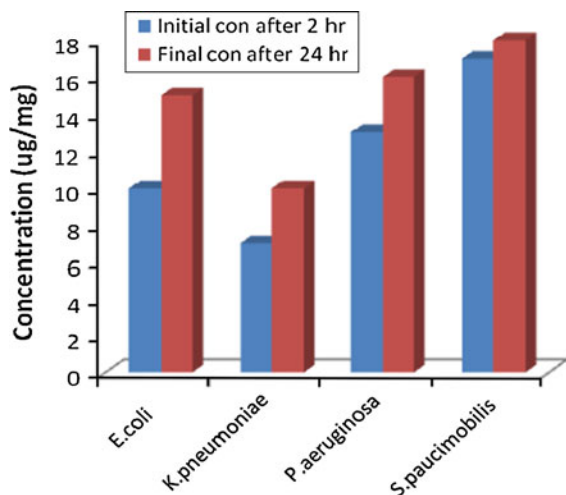


**Fig. 12** Leakage of proteins from ESBL producers after the treatment of ZnO NPs+  $\beta$ -lactam antibiotics

successfully accelerates the leakage of reducing sugars from bacterial cytoplasm.

When identical procedure was applied for protein estimation at the same synergistic concentrations then ZnO NPs also elevated protein leakage from membrane of all bacteria (Fig. 12). Initially, in control, protein leakage was 10, 7, 13, 17  $\mu\text{g}/\text{mg}$  but in treated samples it was found to be 12, 8, 15, 18  $\mu\text{g}/\text{mg}$  and after 4 h it was 15, 10, 16, 18  $\mu\text{g}/\text{mg}$ . The reason for elevated concentrations may be that all bacteria are Gram -ve which possess a membrane for a selective permeability barrier and protect bacteria from harmful agents. The membrane is asymmetric, i.e., outer leaflet composed of lipopolysaccharides whereas inner leaflet contains closely packed phospholipid chain by providing the selective permeability barrier to gram negative bacteria. But the results of synergy study revealed that ZnO NPs+ antibiotic combination enhanced permeability of membrane for reducing sugars and proteins into cell. Still it is a mystery where the damage takes place to the lipopolysaccharides and membrane proteins, and to elucidate the mechanism of synergistic effect more elaborate experimental evidence is needed.

## Conclusion

The synthesized ZnO NPs +  $\beta$ -lactam antibiotics exhibited enhanced synergistic biocidal activity

against all isolated potent clinical ESBL producers and can act as drug carrier to overcome emerging antibiotic resistance. ZnO NPs may be considered as a valuable adjuvant in combination therapy of cefotaxime, ampicillin, ceftriaxone, cefepime and found to be more abrasive by contributing mechanical damage to cell membrane. Though the research findings look preliminary but it provides helpful insight for the development of novel antimicrobial agents for UTI treatment. To elucidate the mechanism of synergistic antibacterial effect there is a need of more elaborate experimental evidences and presently we are working toward this end.

**Acknowledgments** One of the authors RMB gratefully acknowledges the Department of Science and Technology (DST), New Delhi, India for financial assistance in the form of Fellowship through the grant [F.N: SR/WOS-A/LS-305/2010] to carry out this study.

## References

- Baker C, Pradhan A, Pakstis L, Pochan DJ, Shah SI (2005) Synthesis and antibacterial properties of silver nanoparticles. *J Nanosci Technol* 5:244–249
- Barbaru S, Davir R, Alexander P, Sithes L, William TC, Ilya R (2008) A natural history of botanical therapeutics. *Metabol Clin Expt* 57(1):3–9
- Bauer AW, Kirby WMM, Sherris JC, Turch M (1966) Antibiotic susceptibility testing by a standard single disc method. *Am J Clin Pathol* 45:494–496
- Bennet PM (2008) Plasmid encoded antibiotic resistance: acquisition and transfer of antibiotic resistance genes in bacteria. *Br J Pharmacol* 153:347–357
- Bradford M (1976) A rapid and sensitive method for the quantification of microgram quantities of protein utilizing the principle of protein-dye binding. *Anal Biochem* 72:248–254
- Brayner R, Ferrari-Iliou R, Brivois N, Djedit S, Benedetti MF, Fievet F (2006) Toxicological impact studies based on *Escherichia coli* bacteria in ultrafine ZnO nanoparticles colloidal medium. *Nano Lett* 6(4):866–870
- Bruins RM, Kapil S, Oehme SW (2000) Microbial resistance to metal in the environment. *Ecotoxicol Environ* 45:198–207
- Faddin FJ (1980) Biochemical tests for identification of medical bacteria, vol 4. Williams and Williams Co., Baltimore, pp 518–538
- Fernandez F, Neves P, Gemeiro P, Loura LMS, Prieto M (2007) Ciprofloxacin interaction with bacterial protein OmpF: modeling of FRET from a multi-tryptophan protein trimer. *Biochem Biophys Acta* 1768:2822–2830
- Gleiter (2000) Nanostructured materials basic concepts. *Acta Mat* 48:1–12
- Huang JY, Liu YX, Liu T, Gan X, Liu XJ (2009) A nitric oxide biosensor based on the photovoltaic effect of nano titanium dioxide on haemoglobin. *J Anal Chem* 64:735–737

- Huet AA, Rayagade JL, Mendiratta K, Seo SM, Kaatz GW (2008) Multidrug efflux pump over expression in *Staphylococcus aureus* after single and multiple in vitro exposure to biocides and dyes. *Microbiol* 154:3144–3153
- Jones N, Ray B, Ranjit KT, Manna AC (2008) Antibacterial activity of ZnO nanoparticle suspensions on a broad spectrum microorganisms. *FEMS Microb Lett* 279:71–76
- Kim SJ, Eunye K, Kyeong NY, Kim J, Park SJ, Lee HJ, Kim SH (2007) Antimicrobial effects of silver nanoparticles. *Nanomedicine* 3:95–101
- Kumor SA, Chen S (2008) Nanostructured ZnO nanoparticles in chemically modified electrodes for biosensor applications. *Anal Lett* 41:141–158
- Langer R (2001) Drug delivery—drugs on target. *Science* 293:58–59
- Li W, Xie X, Shi Q, Zeng H, Yang Y, Chen Y (2009) Antibacterial activity and mechanism of silver nanoparticles on *E. coli*. *Appl Microbiol Biotechnol* 5:1–10
- Major S, Kumar S, Bhatnagar M, Chopra KL (1986) Effect of hydrogen plasma treatment on transparent conducting oxides. *Appl Phys Lett* 49:394–398
- Marones JR, Elechiguerra JL, Camacho A, Holt K, Kouri JB, Ramirez JT, Yacaman MJ (2005) The bactericidal effect of silver nanoparticles. *Nanotechnology* 16:2346–2353
- Maskell R (1982) Diagnosis of urinary tract infections, its causes and consequences. In: *Urinary tract infection. Curr Top Infect Series* 3M Edward Arnold. London, pp 21–41
- Miller G (1959) Use of dinitrosalicylic acid reagent for determination of reducing sugars. *Anal Chem* 31:426–429
- Muhammad R, Baksh S, Abdus S, Khan GM, Muhammad J (2004) Comparative study of various growth media in isolation of urinary tract pathogens. *Gomal J Med Sci* 2(1):16–19
- Nicole MP, Harding GK, Norris M (1988) Localization of urinary tract infection in elderly institutionalized women with asymptomatic bacteriuria. *J Infect Dis* 157(1):65–70
- Noei H, Qiu H, Wang Y, Loffler E, Woll C, Muhler M (2008) The identification of ZnO nanoparticles by infrared Spectroscopy. *Phys Chem* 10:7092–7097
- Padmavathy N, Vijayaraghvan R (2008) Enhanced bioactivity of ZnO nanoparticles—an antimicrobial study. *Sci Technol Adv Mater* 9:1–7
- Pal S, Tak YK, Joon MS (2007) Does the antibacterial activity of silver nanoparticles depends on the shape of nanoparticle? A study of the Gram-negative bacterium *Escherichia coli*. *App Env Microbiol* 73(6):1712–1720
- Park H, Go H, Kalme S, Mane RS, Han SH, Yoon MY (2009) Protective antigen detection using horizontally stacked hexagonal ZnO platelets. *Anal Chem* 81:4280–4284
- Pen G (2009) Characterization of copper oxide nanoparticles for antimicrobial applications. *J Antimicrob Agents* 33:587–590
- Ping L, Juan L, Changzhu W, Quingsheng W, Jian L (2005) Synergistic antibacterial effect of beta-lactam antibiotics combined with silver nanoparticles. *Nanotech* 16:1912–1917
- Raffi M, Hussain F, Bhatti TM, Akther JI, Hameed A, Hasa MM (2008) Antibacterial characterization of silver nanoparticles against *E. coli* ATCC-15224. *J Mater Sci Technol* 24(2):192–196
- Roy K, Mao H, Huang S, Leong K (1999) Oral gene delivery with chitosan–DNA nanoparticles generates immunologic protection in a murine model of peanut allergy. *Nat Med* 5:387–391
- Ryan BM, Dougherty TJ, Beaulieu D, Chaung J, Dougherty BA, Barret JF (2001) Efflux in bacteria: what do we really know about it? *Expert Opin Invest Drugs* 10:1409–1422
- Sawai J (2003) Quantative evaluation of antimicrobial activities of metallic oxide powders (ZnO, MgO and CaO) by conductimetric assay. *J Microbiol Methods* 54:177–182
- Sharma VK, Yungard RA, Lin Y (2009) Silver nanoparticle on *E. coli*. *Adv Colloid Interf Sci* 145:83–96
- Thati V, Roy AS, Ambika Prasad MVN, Shivannavar CT, Gaddad SM (2010) Nanostructured zinc oxide enhances the activity of antibiotic against *Staphylococcus aureus*. *J Biosci Tech* 1(2):64–69
- Tiller (2001) Designing surfaces that kill bacteria on contact. *Proc Natl Acad Sci USA* 98:5981–5987
- Vaseastha A, Dimova-Malinovaska D (2005) Nanostructured and nanoscale devices, sensors and detectors. *Sci Technol Adv Mater* 6:312–318
- Wang ZG, Zu XT, Zhu S, Wang LM (2006) Green luminescence originates from surface defects in ZnO nanoparticles. *Phys E: Low Dimen Sys Nano* 35:199–202
- Wren C, Nie S (1998) Quantum dot bioconjugates for ultra sensitive nonisotopic detection. *Science* 281:2016–2018
- Yu J, Grinius L, Hooper DC (2002) Nor A functions as a multidrug efflux protein in both cytoplasmic membrane vesicles and reconstituted proteo liposomes. *J Bacteriol* 184:1370–1377